Charmless hadronic B-decays at BABAR and BELLE

N. Arnaud

CHARMLESS HADRONIC B-DECAYS AT *BABAR* AND Belle

N. ARNAUD, representing the *BABAR* and Belle collaborations
Laboratoire de L'Accélérateur Linéaire, IN2P3/CNRS et Université Paris Sud XI, F-91898 Orsay Cedex, France

We report recent results for charmless hadronic B decays from the B-factories. Three *BABAR* analyses are presented: $B \to \phi\phi K$; $B^+ \to \rho^0 K^{*+}$ and $B^+ \to f_0(980) K^{*+}$; inclusive $B \to XK^+$, XK^0 and $X\pi^+$ beyond the charm threshold. Two Belle results are described: search for the $X(214)$ through charmless rare B decays; first measurement of inclusive $B \to X_s\eta$.

1 Introduction

Charmless hadronic B decays are rare processes which branching fractions (BFs) are mostly in the $10^{-6} - 10^{-5}$ range. Yet, about 100 decay modes have been measured [1] with a significance $\geq 4\sigma$, mostly by the B-factories. Indeed these modes allow one to probe the Standard Model of particle physics (SM). The processes are dominated by $b \to u$ trees and $b \to s, d$ gluonic penguins. As the trees are suppressed by the Cabibbo-Kobayashi-Maskawa mechanism [2], the penguins amplitudes are often significant or even dominant. Such loops are ideal places to look for New Physics (NP) as yet-unknown heavy particles could contribute to these decays and yield amplitudes that are significantly different from the SM ones. Moreover, interferences between amplitudes accommodate searches for CP violation and allow relative phase measurements through Dalitz Plot (DP) analysis. Finally, studying such decays helps testing predictions from factorization, perturbative QCD, SU(3) flavour symmetry, etc.

These proceedings review recent results[3,4,5,6,7] from the *BABAR* [8] and Belle [9] experiments which took data during the past decade at the high luminosity$B$-factories PEP-II [10] and KEK-B [11]. Unless otherwise noted, the first uncertainty quoted for a result is statistical and the second systematic. Charge-conjugate states are assumed throughout this document.

2 Analysis techniques

When studying charmless hadronic B decays, the signal is usually small relatively to a large background coming from the production of light quark pairs ($e^+e^- \to q\bar{q}$ with $q = u, d, s, c$: the 'continuum') and other B decays. Correctly reconstructed B decays are selected using two kinematical variables computed in the center-of-mass (CM) frame: the energy-substituted mass $m_{\rm ES} = \sqrt{\left(E_{\rm beam}^{\rm CM}\right)^2 - \left(p_B^{\rm CM}\right)^2}$ (Belle: M_{bc}) which peaks at the B mass, and the energy difference $\Delta E = E_B - \sqrt{s}/2$ that peaks at 0 ($\sqrt{s}$ is the total CM energy). Multivariate analyses combining event-shape variables computed in the CM frame are used to separate B decays ('spherical' as the $B\overline{B}$ pairs are almost produced at rest) from continuum events ('jet-like' as more kinetic energy is available for these decays). Several exclusive or inclusive B background decays are studied and then grouped in classes with similar kinematics and topological properties. These event categories are used in an unbinned extended likelihood fit which combines several discriminating variables and is usually conducted to compute the contributions of the different event categories included in the analysis. The '$B_{\rm reco}$' technique is another way to fight against background. In this case, one of the two B mesons produced in the event is fully reconstructed through exclusive hadronic ($B \to D^{(*)}Y^{\pm}$ where $Y^{\pm}$ is a combination of hadrons) or semi-leptonic ($B \to D^{(*)}l\nu_l$) decays. For each of these channels, Monte-Carlo simulations allow one to compute their purity and efficiency. Depending on the analysis needs, samples favouring either of these criteria can be selected by choosing a subset of the numerous '$B_{\rm reco}$' modes reconstructed in data.

3 Results

3.1 $B \to \phi\phi K$ (BABAR)

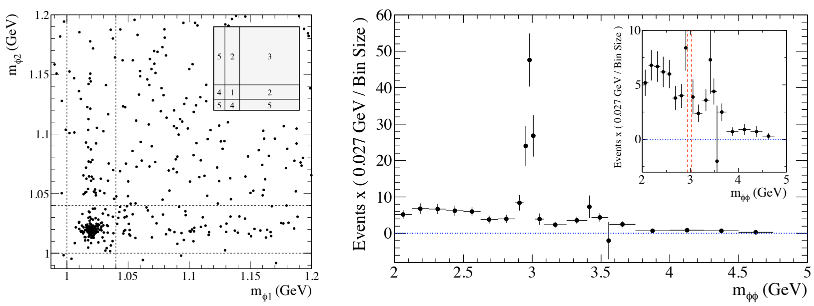

Figure 1: Left plot: signal-enhanced distribution of the selected data in the $m_{\phi 2}$ vs. $m_{\phi 1}$ plane. 5 zones have been defined in this plane (see inset) to measure the signal yield and the contributions of the 4 peaking B background categories. Right plot: fitted $B \to \phi\phi K^+$ yield as a function of the $\phi\phi$ invariant mass. The η_c resonance is clearly visible whereas there is no sign of the χ_c resonances in the two narrow bins around 3.5 GeV/c^2.

The final state $\phi\phi K$ occurs through either a one-loop 'penguin' $b \to s\bar{s}s$ transition or the $b \to c\bar{c}s$ tree-level decay $B \to \eta_c K$ with $\eta_c \to \phi\phi$. Therefore, these two amplitudes can interfere if the $\phi\phi$ invariant mass $m_{\phi\phi}$ is close to the η_c resonance. In the SM, no CP violation is expected from this effect as the relative weak phase difference between the two amplitudes is approximately 0. Conversely, measuring a significant direct CP asymmetry in this channel[12] would clearly trigger NP contributions to the penguin loop. This analysis uses 464×10^6 $B\overline{B}$ events. The branching fractions measured in the invariant mass range below the η_c resonance ($m_{\phi\phi} < 2.85$ GeV) are $\mathcal{B}(B^+ \to \phi\phi K^+) = (5.6 \pm 0.5 \pm 0.3) \times 10^{-6}$ and $\mathcal{B}(B^0 \to \phi\phi K^0) = (4.5 \pm 0.8 \pm 0.3) \times 10^{-6}$ – the neutral mode had not been previously observed with a significance greater than 5σ. They are consistent with the previous BABAR measurement[13] (now superseded) and larger than (although statistically compatible with) the Belle results[14]. They are also higher than the theoretical predictions[15]. The direct CP asymmetries for the $B^{\pm}$ modes are $A_{CP} = -0.10 \pm 0.08 \pm 0.02$ below the η_c threshold ($m_{\phi\phi} < 2.85\,\mathrm{GeV/c^2}$) and $A_{CP} = 0.09 \pm 0.10 \pm 0.02$ in the η_c resonance region ($2.94 \le m_{\phi\phi} \le 3.02\,\mathrm{GeV/c^2}$). These are consistent with zero, in agreement with the SM. Finally, angular distributions of the $B^+ \to \phi\phi K^+$ decays have been studied. They are consistent with $J^P = 0^-$ in the η_c resonance region and favor $J^P = 0^+$ below.

3.2 $B^+ \to \rho^0 K^{*+}$ and $B^+ \to f_0(980)K^{*+}$ (BABAR)

Several B decays to vector-vector (VV) modes like $B^+ \to \rho^0 K^{*+}$ (not observed prior to this analysis) have been studied. For most of them, there is a discrepancy regarding the longitudinal polarization f_L between the predictions from QCD factorization models ($f_L \sim 1$) and the measurements ($f_L \sim 0.5$). Several attempts to understand this 'polarization puzzle' [16] have been made, either within or beyond the SM. This analysis uses a sample of $(467 \pm 5) \times 10^6$ $B\overline{B}$ pairs and supersedes the previous BABAR results. It reports measurements of the branching fraction $\mathcal{B}(B^+ \to \rho^0 K^{*+}) = (4.6 \pm 1.0 \pm 0.4) \times 10^{-6}$ (first observation with a 5.3σ significance, compatible with theoretical predictions), longitudinal polarization $f_L = 0.78 \pm 0.12 \pm 0.03$ (both consistent with the theoretical predictions and with the measured values for the two other $K^*\rho$ modes) and direct CP-violation asymmetry $A_{CP} = 0.31 \pm 0.13 \pm 0.03$ for the decay $B^+ \to \rho^0 K^{*+}$ such as measurement of the branching fraction $\mathcal{B}(B^+ \to f_0(980) K^{*+}) = (4.2 \pm 0.6 \pm 0.3) \times 10^{-6}$ and direct CP-violation asymmetry $A_{CP} = -0.15 \pm 0.12 \pm 0.03$ for the mode $B^+ \to f_0(980) K^{*+}$ which shares the same final states (assuming a branching fraction of 100% for $f_0(980) \to \pi^+\pi^-$).

3.3 Inclusive $B \to XK^+$, XK^0 and $X\pi^+$ beyond the charm threshold (BABAR)

For these decays, theoretical models [18] predict enhancements up to one order of magnitude of the branching fractions with respect to the SM if NP enters in the loop diagrams. This analysis uses 383×10^6 $B\overline{B}$ pairs out of which 2×10^6 events are reconstructed using the hadronic $B_{\rm reco}$ selection technique. Partial branching fractions above the end point for decays to charmed mesons – the momentum p^* of the candidate hadron greater than 2.34 (2.36) GeV/c for kaons (pions) in the $B_{\rm sig}$ rest frame – are reported: $\mathcal{B}(B \to XK^+,\ p* > 2.34\ \text{GeV/c}) = (1.2 \pm 0.3 \pm 0.4) \times 10^{-4} < 1.9 \times 10^{-4}$ at 90% C.L.; $\mathcal{B}(B \to XK^0,\ p* > 2.34\ \text{GeV/c}) = (1.9 \pm 0.5 \pm 0.5) \times 10^{-4} < 2.9 \times 10^{-4}$ at 90% C.L.; $\mathcal{B}(B \to X\pi^+,\ p* > 2.34\ \text{GeV/c}) = (3.7 \pm 0.5 \pm 0.6) \times 10^{-4}$, a decay observed inclusively independently of known exclusive modes. These results are in agreement with the SM and exclude large enhancement due to NP. In addition, no direct CP-asymmetry is observed in the charged modes: $A_{CP}(B \to XK^+) = 0.57 \pm 0.24 \pm 0.05$ and $A_{CP}(B \to X\pi^+) = 0.10 \pm 0.16 \pm 0.05$.

3.4 Search for the $X(214)$ through charmless rare B decays (Belle)

The goal of this analysis is to search for a light scalar or vector particle decaying into a pair of muons. Such X particle could help understanding recent astrophysical observations[19]. Moreover, the HyperCP collaboration has reported the observation of 3 events $\Sigma^+ \to pX(\to \mu^+\mu^-)$ with a mass of 214.3 MeV/c^2 and a lifetime around 10^{-14} s. Two rare decay modes ($B^0 \to K^{*0}X$ and $B^0 \to \rho^0 X$ are searched in a dataset of 657×10^6 $B\overline{B}$ events; branching fractions in the range $10^{-9} - 10^{-6}$ are expected[20] for a sgoldstino of mass 214 MeV/c^2. Two techniques have been used to evaluate the background yield in the signal box defined using the variables M_{bc} and ΔE. The first one consists in counting the number of selected events using MC samples about 3 times larger than the dataset; in the second approach, the number of events is fitted using parameterizations based on sidebands. As a cross-check, various MC distributions are compared to those computed using a small fraction of the data. Finally, no signal is observed and frequentist upper limits are derived: $\mathcal{B}(B^0 \to K^{*0}X) < 2.26\,(2.27) \times 10^{-8}$ and $\mathcal{B}(B^0 \to \rho^0 X) < 1.73\,(1.73) \times 10^{-8}$ for a scalar (vector) X particle decaying into two muons with a lifetime smaller than 10^{-12} s. This rules out some models for a sgoldstino interpretation of the HyperCP observation.

3.5 First measurement of inclusive $B \to X_s\eta$ (Belle)

This study is motivated by the results of inclusive $B \to X_s\eta'$ analysis which show an unexpectedly large branching fraction and a spectrum which peaks at high mass[21]. It uses as well 657×10^6 $B\overline{B}$ events and is based on a pseudo-inclusive method: the X_s is reconstructed in 18 exclusive channels containing a K^+ or a $K^0_s(\to \pi^+\pi^-)$ and up to 4 pions of which at most 1 is a $\pi^0(\to \gamma\gamma)$. For $m_{X_s} < 2.6$ GeV/c^2, the $B \to X_s\eta$ measured branching fraction is $[26.1 \pm 3.0\,^{+1.9}_{-2.1}\,^{+4.0}_{-7.1}] \times 10^{-5}$, where the last error comes from the modeling of the X_s system with PYTHIA. This result is consistent with the known decays $B \to K\eta$ and $B \to K^*(892)\eta$. Over half of the events (7σ significance) are located in the high-mass region ($m_{X_s} > 1.8$ GeV/c^2), which was not covered by previous exclusive measurements. Using the 13 modes for which the B flavor is given by the final state, the direct CP-asymmetry can be computed: $A_{CP} = -0.13 \pm 0.04\,^{+0.02}_{-0.03}$ which is consistent with predictions. The m_{X_s} spectrum shapes and branching fractions are comparable for the η and the η', which rules out the hypothesis of specific η' mechanisms.

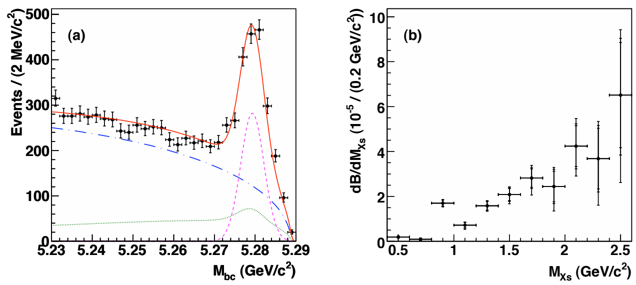

Figure 2: Left: M_{bc} distribution for the full mass range; the points are the data, the solid red line the overall fit function, the magenta dashed line the signal, the green dotted line the $b \to c$ background and the blue dash-dotted the continuum. Right: differential branching fraction as a function of m_{X_s}.

Acknowledgments

I'd like to thank E. Ben-Haim and A. Gaz for their comments on my talk and the proceedings.

References

1. D. Asner *et al*, arXiv:1010.1589 [hep-ex]; http://www.slac.stanford.edu/xorg/hfag
2. M. Kobayashi and T. Maskawa, *Prog. Theor. Phys.* **49**, 652 (1973).
3. J.P. Lees *et al*, *Phys. Rev.* D **84**, 012001 (2011).
4. P. del Amo Sanchez *et al.*, *Phys. Rev.* D **83**, 051101 (2011).
5. P. del Amo Sanchez *et al.*, *Phys. Rev.* D **83**, 031103 (2011).
6. H. J. Hyun *et al*, *Phys. Rev. Lett.* **105**, 091801 (2010).
7. K. Nishimura *et al*, *Phys. Rev. Lett.* **105**, 191803 (2010).
8. B. Aubert *et al.*, *Nucl. Instrum. Methods* A **479**, 1 (2002).
9. A. Abashian *et al.*, *Nucl. Instrum. Methods* A **479**, 117 (2002).
10. PEP-II Conceptual Design Report, SLAC-0418 (1993).
11. S. Kurokawa and E. Kikutani, *Nucl. Instrum. Methods* A **499**, 1 (2003).
12. M. Hazumi, *Phys. Lett.* B **583**, 285 (2004).
13. B. Aubert *et al.*, *Phys. Rev. Lett.* **97**, 261803 (2006).
14. H. C. Huang *et al.*, *Phys. Rev. Lett.* **91**, 241802 (2003); Y. T. Shen *et al.*, arXiv:0802.1547
15. S. Fajfer, T. N. Pham, and A. Prapotnik, *Phys. Rev.* D **69**, 114020 (2004); C.-H. Chen and H.-n. Li, *Phys. Rev.* D **70**, 054006 (2004).
16. See discussion in the *BABAR* article [4] and references therein.
17. B. Aubert *et al.*, *Phys. Rev. Lett.* **97**, 201801 (2006).
18. See discussion in the *BABAR* article [5] and references therein.
19. J. Chang *et al.*, *Nature* **456**, 362 (2008)); O. Adriani *et al.*, *Nature* **458**, 607 (2009).
20. S.V. Demidov and D. S. Gorbunov, *JETP Lett.* **84**, 479 (2007).
21. T. E. Browder *et al.*, *Phys. Rev. Lett.* **81**, 1786 (1998); G. Bonvicini *et al.*, *Phys. Rev.* D **68**, 011101 (2003); B. Aubert *et al.*, *Phys. Rev. Lett.* **93**, 061801 (2004).